ELSEVIER

Catalysis Today 81 (2003) 413–424

CATALYSIS TODAY

www.elsevier.com/locate/cattod

Advances in catalyst development for oxidative ethylbenzene dehydrogenation

S. Geisler [a], I. Vauthey [c], D. Farusseng [c], H. Zanthoff [b,*], M. Muhler [a]

[a] *Lehrstuhl für Technische Chemie, Ruhr-University Bochum, Bochum, Germany*
[b] *Institut de Recherches Sur la Catalyse, CNRS, Villeurbanne, France*
[c] *Degussa AG, Project House Catalysis, Marl, Germany*

Received 28 June 2002; received in revised form 4 December 2002; accepted 17 December 2002

Abstract

Catalyst development for non-stationary redox application is still time consuming. A new method for high-throughput screening of catalysts under non-steady-state conditions is introduced enabling catalyst screening with >50 samples per day. The new method was applied to the oxidative dehydrogenation of ethylbenzene (ODEB) performed by alternately feeding ethylbenzene and oxygen. A highly selective mixed metal oxide catalyst (composition K_2O (0.3 wt.%)/V_2O_5 (16 wt.%)/MgO) was found which converts ethylbenzene into styrene with an overall yield of 80.2% obtained by adding up both the wt.% ethylbenzene and the oxygen pulse. Selectivities in the ethylbenzene pulse amounted up to 98%. Mechanistic investigations reveal that the reaction does not proceed in a typical redox type mode.

Keywords: Catalyst development; Dehydrogenation; Ethylbenzene

1. Introduction

New methods of high-throughput experimentation recently have enabled researchers to enhance the development of new and better performing homogenous and heterogeneous catalysts. Especially for testing of heterogeneous catalysts in recent years a large number of fast tools and reactor set-ups have been reported. For screening of mainly catalyst compositions (first screen) e.g. Maier and co-workers used infrared (IR) thermography to resolve reaction heats for exothermic reactions over a library with 37 materials [1]. Senkan and Ozturk used REMPI to parallel detect benzene yield in dehydrogenation of cyclohexane using an array of catalysts [2]. Symyx company proposed a parallel fixed bed reactor and scanning mass spectrometer for rapid screening [3].

In addition to the optimisation of the principle catalyst formulation reaction conditions as temperature, pressures, stirring, etc. effect the catalytic performance. The study of these parameters generally requires a larger information content from the reaction device and is therefore performed in larger equipment and smaller degree of parallelisation to guarantee scale-up (second screen). Also for this purpose suitable equipment has been developed by several groups [4–6]. These techniques were applied to a range of selective catalytic hydrocarbon oxidation reactions and a number of new formulations were found showing good or better performance compared to earlier developed catalysts, even if no technical application of such catalyst became known up to now.

* Corresponding author.

0920-5861/03/$ – see front matter © 2003 Published by Elsevier Science B.V.
doi:10.1016/S0920-5861(03)00141-X

Table 1
Overview of the performance of ODEB catalysts for non-steady-state operation

Company	Catalyst	Average Y_{Sty} (%) in Etb-pulse only	Average Y_{Sty} (%) in total sequence	Reference
BASF	V-Mg-O	93[a]	?	[22]
ENITechnologie	Bi-V-Mg-O	88	?	[23]
FINA	V-Na-Ca-Fe-Si-Mg-O	97[a]	?	[24]
Present work	K-V-Mg-O	90.2	80.1	
Non-oxidative process	Fe		65	[11]

[a] Valid only for a differential time interval at maximum styrene formation.

For oxidative conversion of hydrocarbons non-steady-state reactor operation has been found to be superior compared to steady-state co-feed flow. Large scale industrial applications are already available, e.g. for butane oxidation (DuPont) or *i*-phthalodinitrile (Lummus). The performance increase can be explained by the fact that the catalyst redox state, which determines the catalytic performance, can be adjusted and applied in its optimum range. Furthermore, the presence of non-selective short-lived oxygen species on the catalyst surface favouring total oxidation is minimised [7,8]. However, the optimisation of these catalyst properties is very time consuming. Until today, no method existed to study these parameters in a fast mode. In the present work, a novel high-throughput method to investigate redox properties of mixed metal oxide catalysts using non-steady-state operation is presented. The performance of the new method is demonstrated applying the oxidative dehydrogenation of ethylbenzene (ODEB) to styrene as test reaction.

Industrial styrene production [9] is based on non-oxidative dehydrogenation of ethylbenzene (Etb) over potassium doped ferric oxide catalysts at temperatures below 900 K. Selectivities exceeding 95% are obtained at equilibrium limited conversions below 70% ($Y_{Sty} \approx 67\%$). Higher conversions are only reached by the removal of hydrogen [10–12]. Furthermore, undesired coke formation occurs and energy entry in the process is high.

$$C_6H_5CH_2CH_3 \rightleftharpoons C_6H_5CH{=}CH_2 + H_2$$
$$\Delta H_R = 125\,\text{kJ/mol}$$

Oxidative dehydrogenation of ethylbenzene can be applied to overcome some of the mentioned limitations [13] but selectivity is limited due to undesired total oxidation in the co-feed mode. Recent investigations have shown that applying a non-steady-state operation of multi-component oxide catalysts (cf. Table 1) can significantly enhance selectivity.

$$C_6H_5CH_2CH_3 + \tfrac{1}{2}O_2 \rightarrow C_6H_5CH{=}CH_2 + H_2O$$
$$\Delta H_R = -122\,\text{kJ/mol}$$

In this case, ethylbenzene and oxygen are passed sequentially over the oxide catalyst.

2. Experimental

2.1. Screening strategy and catalyst preparation

An efficient screening strategy was used to reduce the number of experiments to be performed. The V-Mg-O catalyst system was chosen as the basic material. First, three distinct synthesis methods, i.e. impregnation (IM), sol–gel (SG) and citrate (CI) method were screened by varying the V/Mg ratio. In the second generation, promoter effects and loading were studied for the selected synthesis. The number of experiment was reduced by selecting promoter according to knowledge from literature. Finally, combinations of promoters were screened in the third generation.

First generation consisted of 20 pure V-Mg-O catalysts with vanadium contents from 0 to 70%. Catalysts were prepared using impregnation, sol–gel and citrate method. The catalysts were screened for their performance in non-steady-state ODEB and optimum vanadium contents were chosen for further catalyst optimisation. (Notation: 16VMgO = V_2O_5 (16 wt.%)/MgO.)

Second generation consisted of 48 solids of the type Me-V-Mg-O. The additives Me determined for doping were divided into eight "performance" groups. One element of each group (Me = K (Na, Cs), Sr (Ca, Ba), Nb (Ta), Mo (Cr, W), Bi (Sb), La (Ce), Co (Fe, Ni) and Pt (Pd)) was chosen. Catalysts with low and high loading varying from 0.1 to 5.0 wt.% were prepared, typically 200 mg each. IM- and CI-methods were chosen for scale-up purposes.

Third generation catalysts (14 samples) were prepared by exchanging Me within one additive group and by combining two well performed additives to one catalyst Me_1-Me_2-V-Mg-O.

2.1.1. Preparation methods

2.1.1.1. Impregnation. $(NH_4)_2CO_3$ was added to an aqueous solution of $Mg(NO_3)_2$ stirred at 343 K and pH 7. The resulting solid ($MgCO_3 \times H_2O$) was dried and calcined in oxygen at 937 K (after Kung and Chaar [14]). The resulting MgO powder was added to an aqueous solution of ammonium vanadate at 340 K. After 2 h stirring the suspension was evaporated to dryness. The resulting solid was calcined in air at 873 K for 6 h. The solid was pressed, crushed and sieved to obtain the fraction of 250–355 μm.

2.1.1.2. Sol–gel method. The sol–gel method is based on the low temperature hydrolysis and condensation of hydrolysable precursors $[Mg(OR)_2]_4$ and $[VO(OR)_3]_2$ (OR = $OCH(CH_3)CH_2OCH_3$). The alkoxides resulted in a precursor $\{Mg[VO(OR)_3]_n\}_m$. After gelation the materials were dried and calcined in air at 873 or 1073 K.

2.1.1.3. Citrate method. NH_4VO_3 was dissolved in an aqueous solution of citric acid. After mixing the aqueous solution of $Mg(NO_3)_2$ with the solution of NH_4VO_3 additional citric acid was dispersed in it. The solution was stirred at 393 K to complete vapour evaporation with V/Mg desired ratios. The obtained foams were calcined. Doped samples were prepared by addition of nitrate solutions of respective compounds K, Sr, Nb, Mo, Bi, La, Co, Pt (group leader) or a, Ba, Cs, Na, Pd prior to calcination.

First generation catalysts were prepared using conventional equipment. Subsequent generations were prepared using an automated Zinsser dispenser.

2.2. High-throughput screening set-up

The novel automated equipment [15] consists of eight sequentially alternating quartz reactors, which can be filled with up to 100 mg catalyst. Three gases and two different vaporised liquids can be directed into each reactor at a maximum temperature of 1100 K. The time dependent analysis of reaction products is performed at the reactor outlet by using a quadruple mass spectrometer (BALZERS QMA 125).

A reactor is selected sequentially for the execution of the measurements. After the reactor selected a furnace unit is moved to the reactor for heating up under oxidative conditions. Subsequently, the desired experiments take place. After termination of the desired measurement, the furnace is removed and the roundabout turns automatically for the investigation of the next catalyst into the desired position. Continuously operating, more than 50 catalysts can be tested per day at a single reaction condition (*T*, flow, gas composition).

2.3. Catalyst testing

The catalyst libraries were tested in a non-steady-state mode concerning its catalytic performance in relation to the ODEB by the presented reactor system. Ethylbenzene and oxygen are passed sequentially over the oxide catalyst (cf. Fig. 1). The reaction 'time' of every catalyst (60 mg) amounted to 15 redox cycles plus 5.5 min pre-treatment in oxygen. A mixture of 2.65% ethylbenzene in helium (flow rate 10 ml/min) was used as reaction gas. A mixture of oxygen:inert (Ar + He) = 4:6 (flow rate 10 ml/min) was used for reoxidation. The cycle times were 30 s ethylbenzene and 30 s oxygen. The reaction was performed at atmospheric pressure in the temperature range from 723 to

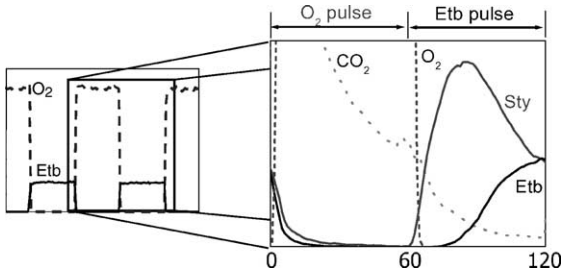

Fig. 1. Non-steady-state operation mode for ODEB.

873 K. Carbon and oxygen mass balances amounted to >95%.

The right part of Fig. 1 shows the courses of the products in the ethylbenzene pulse. In the beginning the high oxidation state of the catalyst causes an increased carbon oxide formation. With increasing time the total oxidation decreases while selective styrene formation becomes dominant. However, ethylbenzene conversion is diminished simultaneously. During the reoxidation pulse (not shown) mainly formation of CO_2 and minor amounts of desorbing styrene and ethylbenzene were observed, all of them decreasing with increasing pulse duration.

2.4. Catalyst characterisation

Bulk and surface properties of selected fresh and ODEB-applied catalysts were determined applying several methods.

2.4.1. Bulk characterisation

XRD pattern were recorded in a 2θ range of 10–100° using a Siemens powder diffractometer D 500 with Cu Kα-radiation.

TPO measurements were performed using a flow of 105 N ml/min O_2 (9.87% in Ar) at a heating rate of 10 K/min and a final temperature of 873 K (m_{cat} = 57 mg).

TG measurements (Chan, model: 2131) are investigated in two steps. First heating in He (106 ml/min, 5 K/min) and cooling down in He (106 ml/min, −20 K/min), second heating in air (75 ml/min, 5 K/min) (m_{cat} = 20 mg). The peaks were identified by analysing the effluent gas stream with a quadrupole mass spectrometer (BALZERS Thermostar).

ESR spectra were recorded on a Jeol Jes-RE2X system at X-band frequency at T = 285 K (microwave frequency: ca. 9.05 GHz; microwave power 5 mW, modulation amplitude of 0.4 mT, sweep time 4 min, sweep width 100 mT, time constant 0.1 s and a modulation frequency of 100 kHz). An estimation of the VO^{2+} concentration was achieved using JOEL Esprit 330 ESR DATA System and using $VOSO_4/Al_2O_3$ (1 wt.% V) as standard experimental error ±15%.

2.4.2. Surface characterisation

DRIFT spectra were recorded with a Nicolet Protégé FTIR spectrometer (Spectra Tech high-temperature chamber). The powdered catalysts were first heated in the DRIFT cell to 773 K in a flow of Ar. Subsequently, DRIFT spectra (800–4400 cm^{-1}) were obtained after cooling to 423 K.

Raman spectra were obtained on a Nicolet Nexus spectrometer (InGaAs detector). Raman scattering was excited with a Nd-YAG laser operated at a wavelength of 1064 nm with a power output of 90 mW.

3. Results

3.1. Catalyst screening

First generation catalysts were tested at temperatures between 723 and 873 K under non-steady-state conditions. Styrene, CO_2 and water were observed as main reaction products CO was observed to a minor extent never exceeding 3.5% in selectivity. With some samples traces of toluene and benzene were detected, too. Only in the first two to three redox cycles the product composition changed. Afterwards always a "semi-steady-state" was reached. The results reported were always taken from the "semi-steady-state" period, usually after the 15th pulse. Styrene was always observed in the first pulses together with CO and CO_2. Fig. 2 illustrates the overall yield to styrene in dependence of the vanadium oxide content in the pure V-Mg-O catalysts and the different preparation methods. Yields up to 70% were obtained (yield calculated for full experiment cycle: 30 s Etb, 30 s O_2). The highest values are obtained at V_2O_5 loadings of 10–30 wt.%. During the ethylbenzene pulse selectivities amounted up to 98% at conversion of >90%. High carbon oxide yields are achieved only during the oxidative regeneration. The differences observed due to the preparation methods applied were less important compared to those originating from the vanadium content. However, it should be mentioned that other calcination conditions (atmosphere, temperature) may result in catalysts which can behave differently for the three preparation methods as has been demonstrated in earlier work, e.g. for propane oxidation.

The second generation catalysts showed improved performance in ethylbenzene dehydrogenation. In Fig. 3 the conversion of ethylbenzene, the selectivity and yield to styrene are reported for 48 tested catalysts at three different temperatures. The highest

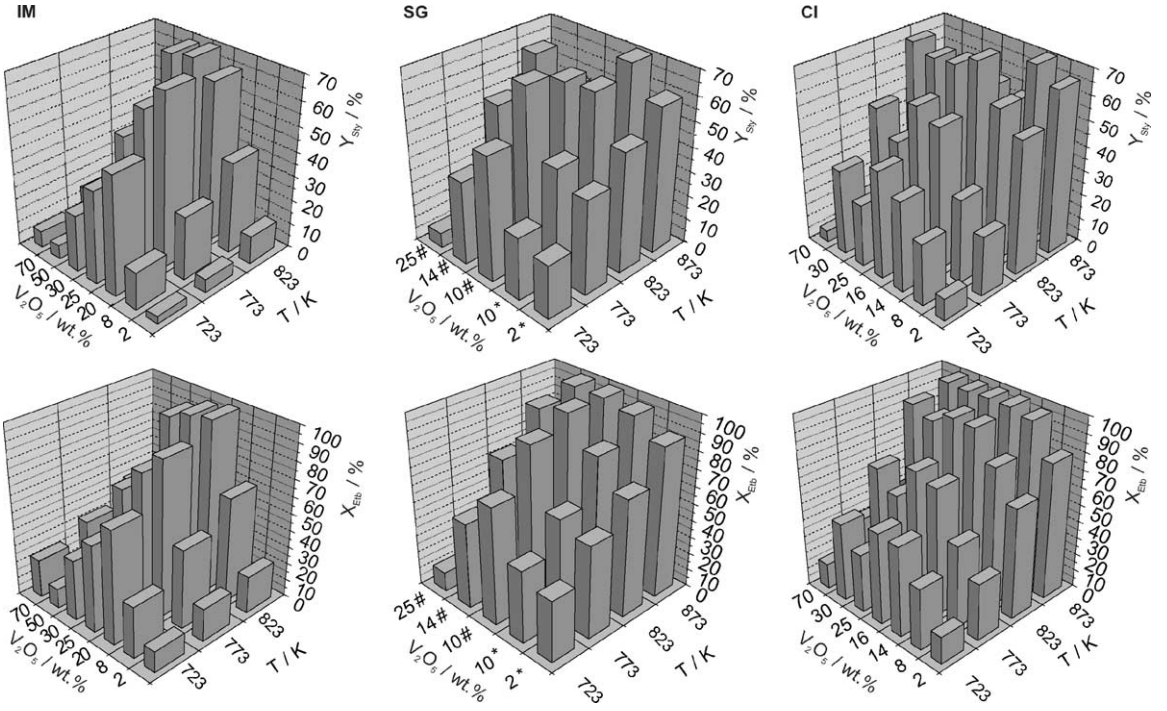

Fig. 2. Overall styrene yields (top) and overall ethylbenzene conversion (bottom) in dependence of the vanadium oxide content and temperature (three different preparation methods: impregnation (IM), sol–gel (SG) and citrate (CI) method; $T_{calcination}$: 823 K, (#) 873 K, (*) 1073 K; cycle times: 30 s Etb + 30 s O_2).

overall yield to styrene of more than 75.3% (cycle time: 30 s Etb/30 s O_2) were obtained for a K (0.5 wt.%)/14VMgO. Selectivities in the ethylbenzene pulse amounted to 96.1% at a conversion of 92.0%.

Using the catalysts of the third generation no improvement in the highest yield to styrene were obtained. However, for the tested temperatures at 723 and 773 K the lowest yields were higher

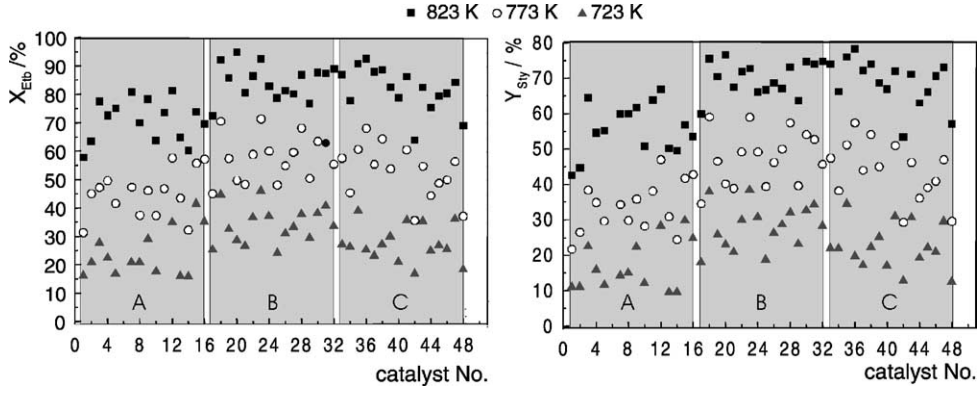

Fig. 3. Ethylbenzene conversion and styrene yields for the second generation catalysts. A = Me-10VMgO, B = Me-14VMgO, C = Me-20VMgO, Me = K, Sr, Nb, Mo, Bi, La, Co or Pt (cycle times: 30 s Etb + 30 s O_2).

Table 2
Maximum and minimum yields to styrene obtained from the catalyst screening of Me-V-Mg-O catalysts in ODEB (cycle times: 30 s ethylbenzene/30 s oxygen; $T = 723$–823 K)

	Maximum yield (%)	Minimum yield (%)
First generation	70	10
Second generation	75	10
Third generation	75	30

compared to the second generation, amounting to 30% (cf. Table 2).

3.2. Influence of cycle times

With increasing cycle times, i.e. increasing pulse duration for ethylbenzene pulse and oxygen pulse, the overall yield and selectivity to styrene increases (cf. Fig. 4). While selectivity steadily increases with increasing cycle duration time its yield passes through a maximum and decreases for high cycle times due to a decrease in ethylbenzene conversion. Maximum yields amounting to $Y_{Sty} = 80\%$ at a pulse duration time of 90 s (cycle time: 90 s Etb/90 s O_2) was obtained for a K_2O (0.3 wt.%)/16VMgO catalyst. The overall selectivity increased from 76 to 91% in the investigated cycle time interval from 30 s Etb/30 s O_2 to 240 s Etb/240 s O_2. Higher yields and selectivities were obtained on balancing the ethylbenzene pulses (not taking into account reoxidation pulse) indicating that part of the ethylbenzene or its products remain adsorbed on the catalyst surface and are burned during the reoxidation pulse. Unexpectedly, the formation of styrene continues for a long time over V-Mg-O catalysts, even if no reoxidation occurs. This is shown in Fig. 5 for the 20VMgO catalyst. After a usual 30 s/30 s (Etb/O_2) pre-treatment at 823 K for 15 pulse sequences the ethylbenzene flow was continued for several thousand seconds. Even after 1200 s continuous ethylbenzene flow significant amounts of styrene were formed. After 350 s flow styrene was the only detectable product.

3.3. Catalyst characterisation

The pure 16VMgO (IM), 20VMgO (IM) and the potassium-modified catalyst K_2O (0.3 wt.%)/16VMgO (IM) that show excellent performance in ODEB and the K_2O (10 wt.%)/16VMgO with low activity were characterised using several bulk and surface techniques.

BET surface areas of the catalysts amounted to 132.2, 122.7, 49.4 and 15.6 m^2/g, respectively.

XRD patterns of the catalysts reveal only the presence of crystalline MgO. Only at high potassium loading the diffraction patterns of KVO_3 (10 wt.% K_2O loading) were obtained (cf. Fig. 6). No crystalline V_2O_5 or mixed V-Mg-O phases were detected. After application to ODEB the 20VMgO catalyst showed a

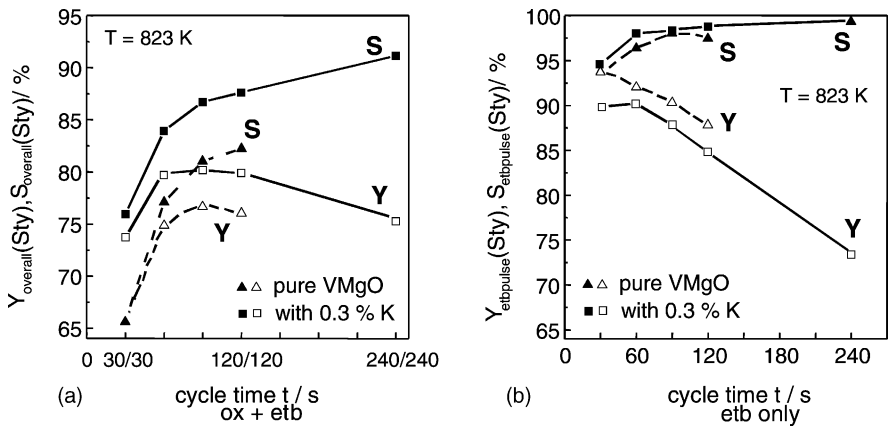

Fig. 4. Dependence of styrene yield and selectivity from the cycle time for 20VMgO (triangles) and K_2O (0.3 wt.%)/16VMgO (squares). (a) Overall cycle of ethylbenzene and oxygen pulse, (b) ethylbenzene pulse only ($T = 823$ K).

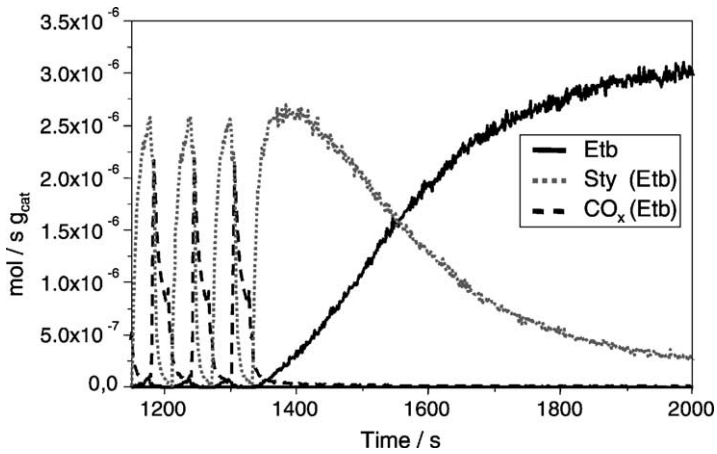

Fig. 5. Amount of ethylbenzene and its reaction products during sequential pulsing of ethylbenzene and oxygen (cycle times: 30 s Etb + 30 s O_2) and for infinite ethylbenzene flow after 1350 s. Amounts of CO_x were corrected for ethylbenzene stoichiometry ($T = 823$ K; $m_{Cat} = 60.5$ mg).

small broad signal at $2\theta = 21.6^\circ$ whereas the signal at 34.9° decreased. However, the identification of this new phase was not possible.

The pure VMgO catalysts did not show any signals in Raman spectroscopy. Only for the high loaded K_2O (10 wt.%)/16VMgO two bands at 937 and 907 cm^{-1} reveal the presence of KVO_3 in agreement with earlier results from Bulushev et al. [16] who investigated K-V-TiO_2 catalysts. It should be mentioned that the high loaded K_2O (10 wt.%)/16VMgO catalyst is nearly inactive (Fig. 7).

DRIFT spectroscopic investigations of fresh MgO reveal the presence of type A and B isolated Mg-OH and Mg-OH-Mg groups mainly on the surface [17]. On the V-Mg-O catalysts the presence of isolated (3725 cm^{-1}) and H bond interacting OH groups (3470 and 3600 cm^{-1}) bound to vanadium ions on the surface can be observed. With increasing vanadium content the

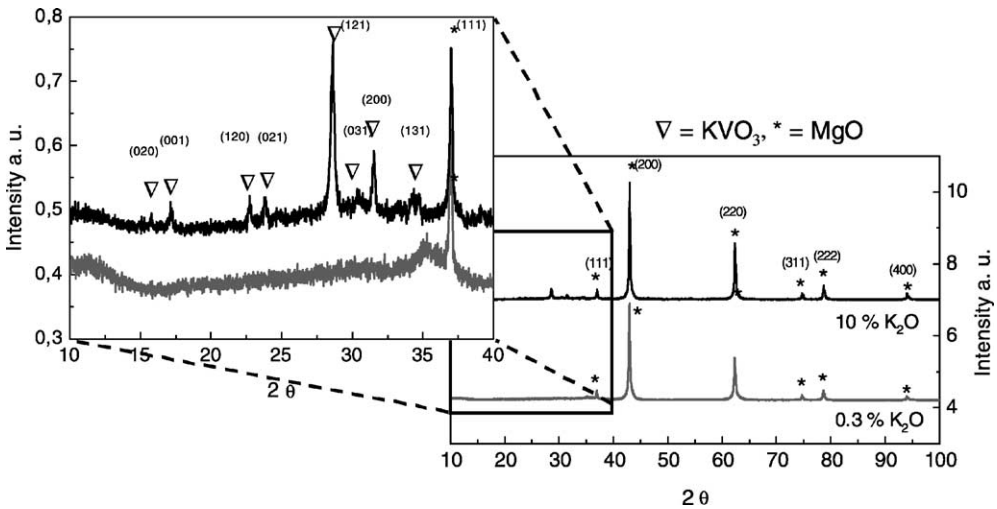

Fig. 6. XRD patterns of K_2O (0.3 wt.%)/16VMgO and K_2O (10 wt.%)/16VMgO.

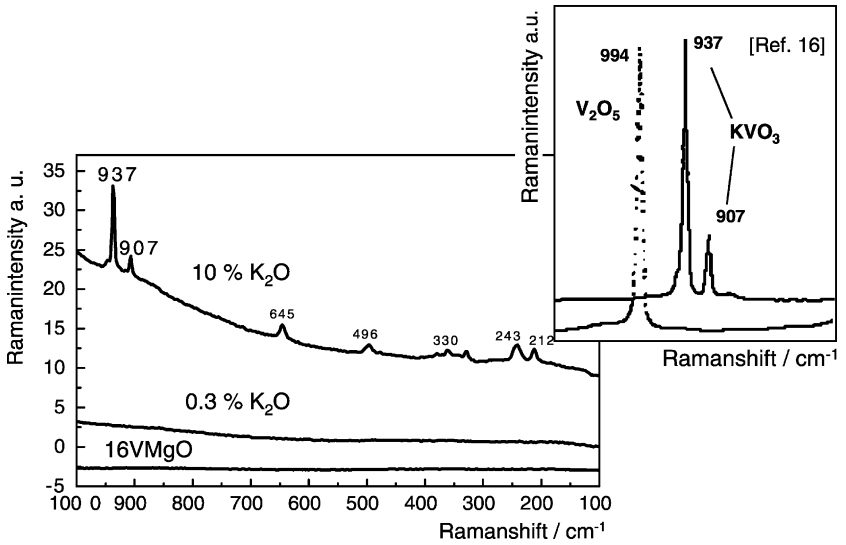

Fig. 7. Raman spectra for (i) 16VMgO, (ii) K_2O (0.3 wt.%)/16VMgO and (iii) K_2O (10 wt.%)/16VMgO.

H bond interacting sites became dominant (cf. Fig. 8a). After treatment of the 20VMgO catalyst with ethylbenzene at 823 K the band at 3470 cm^{-1} diminishes while new phenylic C–H stretching vibration bands at 3098, 3071, and 3030 cm^{-1} appear, indicating that an aromatic hydrocarbon structure is formed on the catalyst surface. Subsequent oxidation re-increases the intensity at 3470 cm^{-1} while the aromatic C–H hydrocarbon vibrations strongly decrease (cf. Fig. 8b).

TPO measurements of the fresh prepared 20VMgO exhibit a small oxygen conversion peak at 600 K only. TPO after treatment of fresh sample for 120 s with ethylbenzene pulse at 823 K results in a large peak at 705 K. TPO after treatment of fresh sample with ethylbenzene at 823 K and subsequent 120 s re-oxidation with oxygen pulse shows that two small peaks remain, one at 600 K and one at 720 K (cf. Fig. 9).

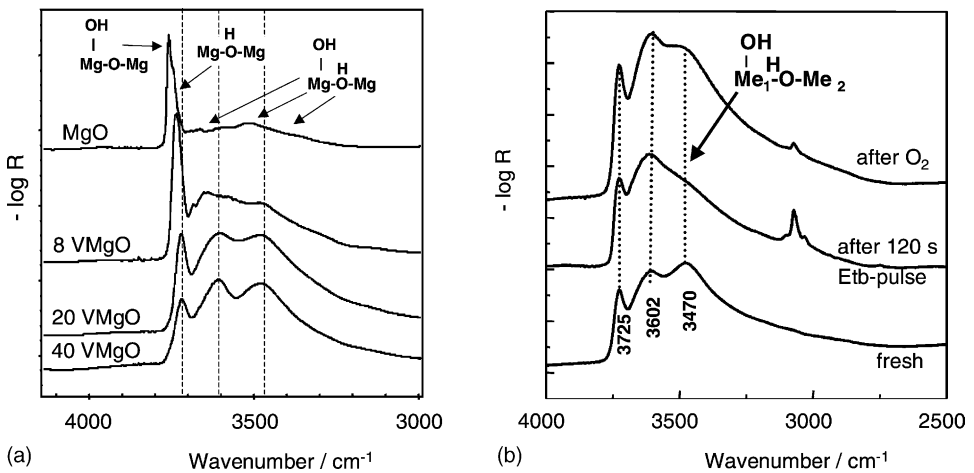

Fig. 8. DRIFT spectra of V-Mg-O catalysts: (a) OH vibrations for different vanadium loading (fresh catalysts) and (b) change in OH vibrations in dependence of the pre-treatment of the 20VMgO catalyst.

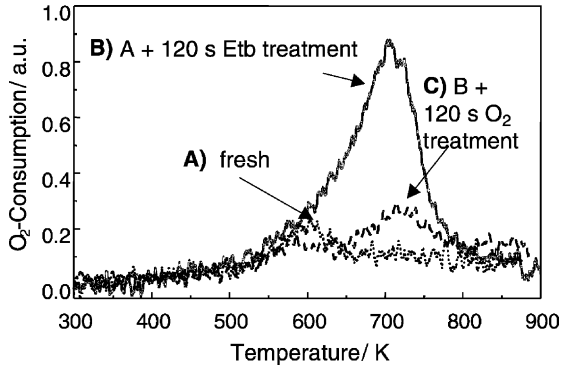

Fig. 9. TPO measurements of 20VMgO: (A) fresh, (B) A + 120 s Etb treatment, (C) B + 120 s O_2 treatment.

Differential thermogravimetry (DTG) was performed using the 20VMgO catalyst after treatment with ethylbenzene. Heating the used catalyst in helium shows three distinct time intervals of mass losses. The first peak occurs at 390 K. Mass spectrometric analysis revealed that mainly water and small amounts of carbon dioxide desorbed from the catalyst. Also the mass loss at 630 K is due to desorption of CO_2 and water. The peaks at 805 K originated from desorbing CO, CO_2 and benzene (traces of water) (cf. Fig. 10). Similar peaks were also obtained when heating in air instead of helium. After cooling down and heating in air one weak peak is found that indicates an uptake of O_2. The maximum of that peak is observed at the same temperature (695 K) as in the TPO measurement (cf. Fig. 9).

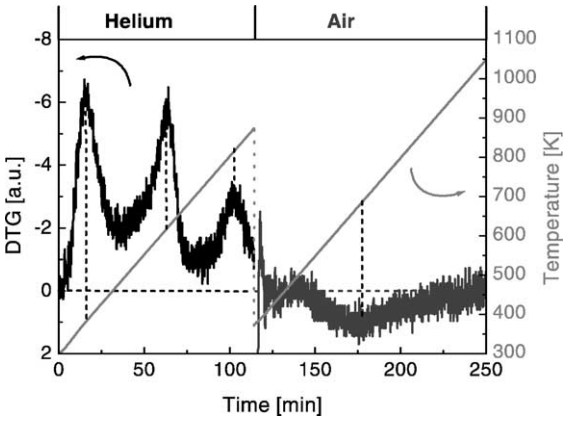

Fig. 10. DTG curves for a 20VMgO catalyst after treatment with ethylbenzene and uptake of oxygen during subsequent heating in air.

Table 3
Spin-Hamiltonian constants for V^{4+} sites in a 20VMgO catalyst at different pre-treatment conditions and total V^{4+} share obtained from quantification

Catalyst	$g_\parallel$	$g_\perp$	$\Delta B_\parallel$ (mT)	$\Delta B_\perp$ (mT)	V^{4+} share (%)
Fresh	1.955	1.965	151	48	72
After 120 s Etb treatment	1.953	1.962	149	48	73
After reoxidation	1.953	1.961	150	47	79

In order to obtain information on the oxidation state of vanadium in the catalysts ESR investigations of the (IM) 20VMgO catalyst were performed as prepared and after pre-treatment with ethylbenzene and subsequent reoxidation. The freshly prepared catalyst reveal the presence of different V^{4+} sites. Clustered vanadium(IV) sites show an isotropic non-resolved signal, which is overlaid by a hfs signal of isolated vanadium(IV) sites. The Spin-Hamiltonian constants are typical for impregnated V-Mg-O catalysts [18]. Quantification revealed that approx. three-fourth of the vanadium in the 20VMgO is present as vanadium in formal 4+ oxidation state. Unexpectedly, the intensity of the signals did not change significantly after treatment with ethylbenzene or reoxidation with oxygen. Also the total amount of V^{4+} sites remained fairly constant (Table 3).

4. Discussion

4.1. Catalyst screening

A new method for fast screening of catalysts to be applied in non-steady-state operation was developed and tested for oxidative dehydrogenation of ethylbenzene. The new method speeds-up the screening procedure by a factor of 10–20. This caused new time consuming bottlenecks to come up which are catalyst preparation and data analysis. The latter is of great importance, because especially for evaluation of non-steady-state experiments mathematical procedures are very complex. Therefore, in order to reduce expenditures here, we used an “intelligent” procedure

to reduce the number of experiments to be performed. This was possible by grouping potential additives according to knowledge from literature. Catalysts were grouped according to their general performance in oxidation catalysis, e.g. acidity reduction (alkaline earth metals), reoxidation (Fe, Co) or main dehydrogenation compounds (Nb, Ta). Only two generations of catalysts were necessary to obtain a new catalyst composition with ODEB performance comparable to earlier patented data.

4.2. Effects of catalyst composition and preparation method

The results from first generation screening show that activity and selectivity of the catalysts strongly depend on the V/Mg ratio. Conversion increases with vanadium content running through a maximum at approx. 10–25 wt.% V content. Also, maximum yields were observed in this range of vanadium content (cf. Fig. 2). This behaviour is typical for V-Mg-O catalysts applied in oxidation [19]. On the other hand, the preparation method only slightly effected the overall performance of the catalysts. However, we can note that the best performance for a given method is obtained with a slightly different V/MgO ratio. The sol–gel method is more adapted to low V contents (<14 wt.%) whereas the IM- and CI-methods are best performing at higher contents (<25 wt.%).

The results for second generation screening are very complex. No clear trend can be identified. The promotion of the V-Mg-O catalysts with alkaline or alkaline earth metal ions, however, always significantly increased selectivity and yield if low loading was applied. This effect was therefore studied in more detail (see below).

4.3. Reaction mechanism

The ex situ infrared spectroscopic investigations reveal that ethylbenzene reacts on V-Mg-O catalysts with acidic OH groups with vibration frequencies around 3470 cm^{-1}. Acidic groups are also involved in the styrene formation as shown by doping with alkali ions. Adding 0.3 wt.% potassium to the V-Mg-O catalyst increases selectivity towards styrene, but slightly reduces activity (conversion). This behaviour was also observed for other vanadium catalysts in aromatics and paraffin oxidation reactions [20,21]. The beneficial effect of small amounts of potassium is yet not clarified. It might be assumed that K increases the electron density in the valence band or increases the local electrostatic potential [20] therefore increasing the desorption rate of the acidic intermediate products before they are totally oxidised or coke the catalyst. Ten weight percent K_2O addition completely deactivates the catalyst. This can be explained by complete coverage of the active vanadium sites by potassium. Ten weight percent K_2O corresponds to 10 theoretical monolayers K atoms in the V-Mg-O catalyst.

In general, vanadium catalysts act as redox sites during catalytic oxidation reactions. This is also the case in ODEB for the fresh catalyst. CO_x and styrene are observed in the first seconds of the first ethylbenzene pulse over all fresh V-Mg-O catalysts. However, the present results give some indication that under "semi-steady-state" conditions, i.e. after all responses to the ethylbenzene and oxygen pulses are similar, the oxidative ethylbenzene dehydrogenation proceeds differently. The formation of styrene under continuous flow conditions of ethylbenzene only (cf. Fig. 5, right part) shows that a larger quantity of ethylbenzene can be converted to styrene than removable oxygen is available in the catalyst. 60 mg of 20VMgO possesses a maximum of 1.33×10^{-4} mol of active oxygen (assuming that each vanadium atom can be formally reduced from V^{5+} to V^{3+}). However, after 1200 s continuous flow of ethylbenzene approx. 8.88×10^{-4} mol of active oxygen should have been removed from the catalyst. This is eight times as much as available. Therefore, it must be concluded that in addition to the redox mechanism a second formation path for styrene exists. This idea is supported by the ESR and TPO investigations.

ESR reveals that the overall oxidation state of the fresh 16VMgO catalyst after calcination is close to 4.25 (75% of vanadium has formal oxidation state 4+). This is also supported by the fact that additional treatment with oxygen (TPO) between 475 and 823 K results in an additional oxygen uptake exactly necessary to fully oxidise the V^{4+} ions in the catalyst to V^{5+}. The freshly calcined K_2O (0.3 wt.%)/16VMgO catalyst therefore contains 6.6×10^{-5} mol of removable oxygen atoms per 60 mg (by reduction of vanadium into formal V^{3+}). The amount of ethylbenzene nearly fully converted into styrene, however, amounted

to 4.0×10^{-5} mol (in 240 s flow). This would reduce the V^{4+}/V^{5+} amount by approx. 60%. ESR spectra, however, reveal no decrease >15%. It should, however, be mentioned that the ESR measurements were performed ex situ and contamination by air cannot be excluded.

TPO of the ethylbenzene treated catalyst (after 120 s Etb; Fig. 9, curve B) reveals that hydrocarbon fragments remain on the surface that can be burned off (CO_2 was detected at the reactor outlet). However, the amount of oxygen applied in the non-steady-state ODEB oxygen pulse was not able to fully clean the surface. This can be seen in a TPO experiment performed after the reoxidation pulse (curve C in Fig. 9) showing a remaining oxygen uptake at 700–750 K. Remaining hydrocarbon fragments can also be identified in the respective DRIFT spectrum (cf. Fig. 8b; 3070 cm^{-1}).

IR, TPO and DTG further show that aromatic hydrocarbon species are strongly adsorbed on the catalyst surface even under reaction temperature conditions. It can be calculated that approx. 20% of all vanadium sites present in the 20VMgO are covered by ethylbenzene species as revealed by quantifying the DTG data. Temperature-programmed desorption of these species, however, predominantly leads to total oxidation products.

It has been frequently proposed that active coke plays an important role in ethylbenzene dehydrogenation over acidic catalysts. This active coke can originate from strong adsorption and polymerisation of produced styrene during oxydehydrogenation with anthraquinone-like structures [10]. Taking into account the above results it might be concluded that surface-bound aromatic species also participate in ODEB over V-Mg-O catalysts.

5. Conclusion

A new high-throughput catalyst screening device was developed which enables to screen catalysts under non-steady-state conditions in a fast way. Up to 50 catalysts can be tested per day for one standard condition. The applicability of the new device was proven in the catalyst development for oxidative dehydrogenation of ethylbenzene to styrene.

After only 300 catalyst and reaction parameter tests, a new catalyst based on the known V-Mg-O system, i.e. K_2O (0.3 wt.%)/16MgO, was found which exhibits high performance in the oxidative dehydrogenation comparable to the best catalysts known from literature and patents. Further improvement of reaction cycle times resulted in an optimised overall styrene yield of 80.2% ($T = 823$ K; cycle times: 90 s Etb pulse, 90 s O_2 pulse). Thus the catalyst development process can be successfully monitored via the presented screening strategy.

Characterisation of selected VMgO and KVMgO catalysts gave hints that the redox state of the catalyst is not sufficiently changed during the non-steady-state ODEB operation. From these results it might be concluded that the non-stationary dehydrogenation of ethylbenzene to styrene over V-Mg-O catalysts does not proceed via a pure redox mechanism. Probably also in this case coke formation on the catalyst surface plays an important role in the reaction mechanism. Further work is going on to elucidate these phenomena.

Acknowledgements

The authors would like to thank Mrs. E. Löffler and Mr. M. Bergmann (Ruhr-University Bochum) for performing the DRIFT and Raman experiments and Dr. S. Grasser for performing the ESR spectroscopy measurements (TU München).

References

[1] A. Holzwarth, H.W. Schmidt, W.F. Maier, Angew. Chem. Int. Ed. 37 (19) (1998) 2644.
[2] S.M. Senkan, S. Ozturk, Angew. Chem. Int. Ed. 38 (6) (1999) 791.
[3] Symyx Technologies, PCT Pat. Appl. WO 99/64160, (1999).
[4] C. Hoffmann, A. Wolf, F. Schueth, Angew. Chem. Int. Ed. 38 (1999) 2800.
[5] D. Wolf, O.V. Buyevskaya, M. Baerns, Appl. Catal. A: Gen. 200 (2000) 63.
[6] O.V. Buyevskaya, D. Wolf, M. Baerns, Catal. Today 62 (2000) 91.
[7] A. Bielansky, J. Haber, Oxygen in Catalysis, Marcel Dekker, New York, 1991.
[8] H.W. Zanthoff, S.A. Buchholz, A. Pantazidis, C. Mirodatos, Chem. Eng. Sci. 54 (1999) 4397.
[9] J. Yoo, Appl. Catal. A: Gen. 142 (1996) 19.
[10] F. Cavani, F. Trifiro, Appl. Catal. A: Gen. 133 (1995) 219.

[11] Fa. ABB Lummus Global SMART Styrene Process, Technology Profile, Bloomfield, NJ, USA.
[12] J. Romantier, M. Bentham, T. Foley, J.A. Valentine, in: Proceedings of the Dewitt Petrochem. Rev., Houston Texas, 1992, p. K1.
[13] W.S. Chang, Y.Z. Chen, B.L. Yang, Appl. Catal. A: Gen. 124 (1995) 221.
[14] H.H. Kung, M.A. Chaar, US Patent 4,777,319 (11 October 1988).
[15] S. Geisler, H.W. Zanthoff, M. Muhler, Chem. Ing. Technol., in press.
[16] D.A. Bulushev, F. Rainone, L. Kiwi-Minsker, A. Renken, Langmuir 17 (2001) 5276.
[17] E. Knötzinger, K.H. Jacob, S. Singh, P. Hofmann, Surf. Sci. 290 (1993) 388.
[18] J. Hanuza, B. Jezowska-Trzebiatowska, W. Oganowski, J. Mol. Catal. 29 (1985) 109.
[19] A. Pantazidis, A. Auroux, J.M. Herrmann, C. Mirodatos, Catal. Today 32 (1996) 81.
[20] J. Zhu, S.L.T. Andersson, J. Chem. Soc., Faraday Trans. I 85 (11) (1989) 3629.
[21] G. Busca, G. Centi, F. Trifiro, J. Am. Chem. Soc. 107 (1985) 7757.
[22] A. Hagemeyer, G. Lauth, T. Lautensack, A. Deimling, US Patent 5,902,918 (11 May 1999).
[23] P. Ingallina, L. Carluccio, C. Perego, G. Del Piero, F. Assandri, Eur. Pat. Appl. 1,160,011 (25 May 2001).
[24] L.F.L. Delorme, F. Martins Mendes Cerejo, J.F. Grootjans, Eur. Pat. Appl. 0,403,462 (14 May 1990).